

## AUDITORY NERVE INPUTS TO COCHLEAR NUCLEUS NEURONS STUDIED WITH CROSS-CORRELATION

E. D. YOUNG\* AND M. B. SACHS

Department of Biomedical Engineering and Center for Hearing Sciences, 505 Traylor Building, Johns Hopkins University, 720 Rutland Avenue, Baltimore, MD 21205, USA

**Abstract**—The strength of synapses between auditory nerve (AN) fibers and ventral cochlear nucleus (VCN) neurons is an important factor in determining the nature of neural integration in VCN neurons of different response types. Synaptic strength was analyzed using cross-correlation of spike trains recorded simultaneously from an AN fiber and a VCN neuron in anesthetized cats. VCN neurons were classified as chopper, primarylike, and onset using previously defined criteria, although onset neurons usually were not analyzed because of their low discharge rates. The correlograms showed an excitatory peak (EP), consistent with monosynaptic excitation, in AN–VCN pairs with similar best frequencies (49% 24/49 of pairs with best frequencies within  $\pm 5\%$ ). Chopper and primarylike neurons showed similar EPs, except that the primarylike neurons had shorter latencies and shorter-duration EPs. Large EPs consistent with end bulb terminals on spherical bushy cells were not observed, probably because of the low probability of recording from one. The small EPs observed in primarylike neurons, presumably spherical bushy cells, could be derived from small terminals that accompany end bulbs on these cells. EPs on chopper or primarylike-with-notch neurons were consistent with the smaller synaptic terminals on multipolar and globular bushy cells. Unexpectedly, EPs were observed only at sound levels within about 20 dB of threshold, showing that VCN responses to steady tones shift from a 1:1 relationship between AN and VCN spikes at low sound levels to a more autonomous mode of firing at high levels. In the high level mode, the pattern of output spikes seems to be determined by the properties of the postsynaptic spike generator rather than the input spike patterns. The EP amplitudes did not change significantly when the presynaptic spike was preceded by either a short or long interspike interval, suggesting that synaptic depression and facilitation have little effect under the conditions studied here. © 2008 IBRO. Published by Elsevier Ltd. All rights reserved.

**Key words:** cross-correlation, ventral cochlear nucleus, synaptic strength.

The definition of neuron types in the cochlear nucleus by Osen (1969) was a seminal observation for research on this nucleus. In the ventral cochlear nucleus (VCN), the

differentiation of spherical and globular bushy cells and their distinction from a heterogeneous population of multipolar cells provided the basic model for the VCN that was elaborated over subsequent years. In this model, the VCN consists of parallel systems of different neuron types, each innervated by auditory nerve (AN) fibers of all best frequencies (BFs) (Osen, 1970b).

As knowledge of the differences in innervation patterns (Osen, 1970a; Cant, 1992) and postsynaptic membrane properties (Oertel, 1983; Manis and Marx, 1991) of VCN neurons accumulated, functional models of neural integration in each parallel pathway were developed. Bushy cells participate in secure synapses with AN fibers so as to provide precise temporal information about AN spike times for the analysis of interaural time difference in the superior olivary complex (e.g. Joris and Yin, 2007; Joris and Smith, in press). Multipolar neurons temporally integrate the activity of AN fibers to provide a stable and robust representation of stimulus spectrum (e.g. Blackburn and Sachs, 1990). Critical to these models was the identification of primarylike (pri) neural response patterns with bushy cells and chopper response patterns with multipolar cells (Rhode et al., 1983; Smith and Rhode, 1987, 1989; Ostapoff et al., 1994; Rhode, in press).

Computational studies identified the strength of the synapses made by AN fibers on VCN neurons as an important variable in determining their response properties (Molnar and Pfeiffer, 1968; Rothman et al., 1993; Hewitt and Meddis, 1993; Joris et al., 1994). Although postsynaptic properties determine the basic features of VCN responses (Banks and Sachs, 1991; Arle and Kim, 1991; Wang and Sachs, 1995; Rothman and Manis, 2003) including phase locking, regularity, and peri-stimulus time (PST) histograms, these properties are strongly modulated by the degree of convergence of AN inputs and their synaptic strengths.

There has been no direct study of the functional strength of synapses between AN fibers and VCN neurons *in vivo*. This information can be obtained from studies of the cross-correlation of spike trains of simultaneously recorded AN fibers and VCN neurons, which is reported here. Cross-correlation has been used in the auditory system to work out neural circuits (Voigt and Young, 1990), to analyze the ensemble representation of stimuli (deCharms and Merzenich, 1996; Eggermont, 2006), to analyze temporal features of the responses to sound (Louage et al., 2005), and to analyze the organization of projections from one level of the system to the next (Miller et al., 2001). Because the organization of AN synapses on CN neurons is relatively simple and much is known about it, it is pos-

\*Corresponding author. Tel: +1-410-955-3164; fax: +1-410-955-1299. E-mail address: eyoung@jhu.edu (E. D. Young).

**Abbreviations:** AN, auditory nerve; BF, best frequency; CM, central mound; DCN, dorsal cochlear nucleus; EP, excitatory peak; EPSC, excitatory postsynaptic current; EPSP, excitatory postsynaptic potential; pri, primarylike; pri-N, primarylike-with-notch; PST, peri-stimulus time; VCN, ventral cochlear nucleus.

sible to interpret the results of cross-correlation at this synapse with some certainty, as opposed to the difficulties posed by unknown circuits in other parts of the auditory system.

Here we show that the cross-correlograms of AN fibers and VCN neurons have the expected properties of short duration, short latency excitatory effects that are tonotopic. Little effect of short-term plasticity was observed. However, cross-correlation was observed only at low sound levels, which raises new questions about the modes of integration of AN activity by VCN neurons at high sound levels.

## EXPERIMENTAL PROCEDURES

Two types of experiment were done using similar preparations: 1) simultaneous recordings from pairs of AN fibers (AN/AN experiments, four cats); 2) simultaneous recordings from AN fibers and VCN neurons (AN/VCN experiments, 14 cats). All surgical and experimental procedures were approved by the Johns Hopkins Animal Care and Use Committee; procedures are in compliance with the U.S. Animal Welfare Act and with Public Health Service policies. Every effort was made to minimize the number of animals used and their suffering.

### Surgical preparation and electrodes

Cats were given atropine (0.03 mg/kg i.m.) to control secretions and anesthetized with ketamine (30–40 mg/kg i.m.). A tracheotomy was performed and a venous cannula was inserted. Anesthesia was maintained by sodium pentobarbital ( $\approx 3$  mg/kg/h i.v., as necessary to maintain areflexia). The cat's temperature was maintained at 39 °C with a feedback-controlled heating pad. Lactated Ringer's was injected i.v. to prevent dehydration. The bulla was vented with a length of small-bore polyethylene tubing to prevent buildup of static pressure in the middle ear.

The skull over the cerebellum was removed and retraction and aspiration of the cerebellum were used to expose the cochlear nucleus. Gentle traction on the cerebellum and small cotton balls placed against the dorsal cochlear nucleus (DCN) were used to expose the AN at the internal meatus. For AN recording, micropipettes filled with 3 M NaCl were used (10–30 M $\Omega$  impedance); for VCN recording, platinum–iridium electrodes were used. Only well-isolated single neurons were studied. In the AN/AN experiments, two micropipettes were placed in the AN in close proximity (<1 mm) in a medial–lateral orientation, so that they might intercept the same bundles of fibers and thus record from fibers with similar BFs. In the AN/VCN experiments the pipette was placed in the nerve and the metal electrode in the VCN. Histology was done in nine of the AN/VCN experiments to locate the electrode tracks. All were in the VCN.

For recording, the cat was placed in a soundproofed chamber. The closed acoustic system was coupled to the ear through a 13 cm ear bar and was calibrated *in situ* with a probe tube placed at the mouth of the ear bar.

### Data acquisition

In experiments involving the VCN, a neuron was isolated on the CN electrode and held while a succession of AN fibers was isolated and studied. Generally it was possible to hold CN neurons for periods of up to an hour or two, whereas AN isolation lasted typically <15 min. We attempted to find fibers with BFs similar to the VCN neuron. The AN/AN experiments were conducted similarly, except that both neurons were in the AN. When a neuron was isolated on one electrode, its BF and threshold were determined manually, as the frequency at which a rate response could

be detected at the lowest sound level. The spontaneous rate class (low, medium, or high) of AN fibers was determined by counting spontaneous spikes over a period of a few s; low spontaneous rates are below 1/s, medium are between 1 and 20/s, and high are above 20/s. For VCN neurons, data for a PST histogram of responses to BF tones at 20–30 dB above threshold were taken (50 ms bursts, 1.6 ms rise/fall, presented once per 500 ms, 200–300 repetitions).

Cross-correlation data consisted of 50 s long periods of spontaneous discharge or discharge driven by a steady tone. Because stimulus-driven rate fluctuations produce artifacts in cross-correlation analysis, as discussed below, the emphasis was on obtaining data at steady discharge rates. Spontaneous activity was used if the rate was sufficient to give enough spikes for the analysis. If a stimulus was presented, it was turned on 10 s before the 50 s data acquisition period was started, to minimize the amount of rate adaptation. If a tone was presented, its frequency was usually set to the BF of the AN fiber in order to emphasize that fiber's contribution to the VCN neuron. As is shown below, significant correlation was only seen at sound levels near threshold, so stimuli were first set a few dB above threshold. If the pair of neurons was held long enough, the stimulus level was raised in 2–10 dB steps until no cross-correlation was seen in an online cross-correlogram. The 50 s data acquisition periods were repeated for each stimulus until the presence or absence of a significant feature in the cross-correlogram was clear (typically 1000–10,000 spikes in both neurons).

In a few cases, broadband frozen (i.e. periodic) noise was used as the stimulus. The noise had an approximately flat spectrum with a bandwidth of 50 kHz and a period of 1 s.

### Cross-correlation analysis

The cross-correlogram is an estimate of the rate of spiking in the presumed postsynaptic neuron (the VCN neuron) as a function of time preceding and following spikes in the presumed presynaptic neuron (the AN fiber), called the *reference neuron* below. Here, spike times were recorded with a time resolution  $h=0.1$  ms, which sets the basic binning of the data. The cross-correlogram  $x(k)$  was computed with a bin resolution  $b=3$ , corresponding to an actual bin width  $bh=0.3$  ms, as follows:

$$x(k) = \frac{\#[A\text{-spike in bin } i, B\text{-spike in bins } i+kb \text{ through } i+kb+b-1]}{N_A bh} \quad (1)$$

where the notation  $\#[\ ]$  means the number of events of the type described within the brackets and a spike is "in bin  $i$ " if the spike occurs at a time in  $(ih, (i+1)h)$ . A-spikes are spikes of the reference neuron, B-spikes belong to the other neuron, and  $N_A$  is the number of A-spikes. Essentially Eqn. 1 corresponds to computing a series of PST histograms for the B neuron centered on the A-spikes and then averaging those histograms. The units of  $x(k)$  are spikes/s.

If A and B discharge independently,  $x(k)$  should fluctuate around  $R_B$ , the average discharge rate of the B neuron. However, rate trends in the data, caused usually by adaptation to an acoustic stimulus, cause the mean value of  $x(k)$  to deviate from  $R_B$ . The effect is small here because stimuli were close to threshold. Because the rate trend is very slow compared with the important features of correlograms (described below), it produces a broad elevation in the correlogram, which appears as a constant offset over the time interval analyzed. For this reason, the mean value of  $x(k)$  is used here as the null value of the correlogram instead of  $R_B$ .

For analysis, *significant features* are considered to be sequences of two or more successive bins of  $x(k)$  that deviate from the mean value by  $\geq 2$  standard deviations. For computing the mean and standard deviation, an iterative process was used in which statistics were computed for bins lying outside features

(deviations from the mean of <2 standard deviations), then the features were redefined, and the process was repeated. Usually this process converged on a fixed number of bins after one to two iterations.

Usually cross-correlograms are interpreted with reference to a correlogram predictor which is a correlogram in which the spikes of one neuron are delayed by an integral number of cycles of any stimulus that is present. In this work, the stimuli are continuous, so a predictor is not relevant, except for the pairs studied with a frozen noise stimulus. In that case, the predictor was computed as the cross-correlogram of the PST histograms of the two neurons to one cycle of the frozen noise stimulus.

### VCN neuron classification

VCN neurons were classified according to the usual scheme based on PST histogram shapes (Blackburn and Sachs, 1989). Neurons were classed as either choppers, pris, or onset neurons. The chop-S (regular) and chop-T (irregular) subtypes of choppers and the strict primarylike and primarylike-with-notch (pri-N) subtypes of primarylike (pri) neurons were recognized, although significant differences related to the subtypes were not found. Because onset neurons produce little or no steady discharge to tones and have no spontaneous activity, they were usually not studied, and subtypes of onset neurons were not identified.

The criteria for classification were similar to the decision tree of Blackburn and Sachs (1989), emphasizing the following: 1) PST histogram shape; 2) regularity of discharge; and 3) first spike latency. Classification data were usually available at 20–30 dB re threshold. In classifying a neuron, all properties were considered simultaneously. In some neurons with high discharge rates, the PST histogram shape and regularity can be equivocal. All neurons become regular at high rates because of refractoriness and pri neurons can produce what appears to be very rapid chopping, again because of refractoriness. In these cases latency was the deciding factor. Fig. 1 shows a scatter plot of minimum first spike latency versus BF for all VCN neurons encountered, showing neurons classed as choppers, pris, and onsets with different sym-

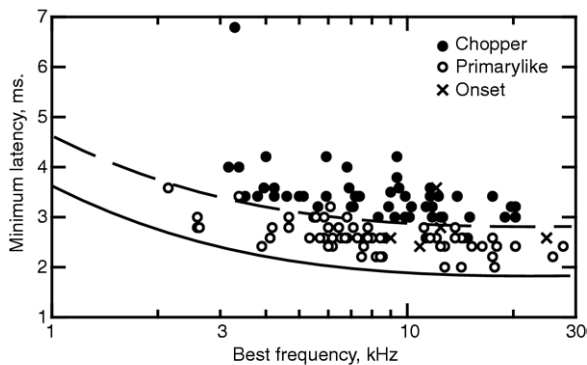


**Fig. 1.** Minimum latencies of VCN neurons separated into chopper, pri (including pri-N), and onset categories, as shown in the legend. Minimum latency is the latency at which the histogram of first-spikes during a tone burst first deviates from spontaneous activity. The latencies have not been corrected for a 0.55 ms acoustic delay in the sound system (Young et al., 1988). Solid and dashed lines are vertically shifted versions of the AN group delay function defined by Goldstein et al. (1971):  $\tau_G = 1.25[1 + (6/f_{BF}^2)]^{1/4}$  where  $\tau_G$  is the delay in ms and  $f_{BF}$  is the BF in kHz. The vertical shift is 0.55 ms (solid line), corresponding to the acoustic delay, and 1.55 ms (dashed line). The dashed line separates pri and chopper neurons, except for a few cases. In those cases, the classification was unequivocal based on the PST histogram and regularity.

bols. Note that choppers have reliably longer latencies (~1 ms) than pri and onset neurons.

Latency data were obtained for a small number of AN fibers. The AN minimum latency was reliably shorter than the latency of simultaneously studied CN neurons or of adjacent CN neurons in the same track, by 0.74 ms for pri neurons (mean of  $N=21$ , range 0.06–1.61, S.D. 0.33) and by 1.13 ms for choppers  $N=14$ , range 0.5–3.16, S.D. 0.65). A complicating factor with AN latencies is that the bandwidth of the AN head stage amplifier (but not the CN amplifier) varied considerably depending on the degree of adjustment of its capacitance neutralization, which changed as the properties of the micropipette changed through a track. Empirically, the range of maladjustment could delay AN spike latencies by up to 0.5 ms.

## RESULTS

### Examples of cross-correlograms

For two independent neurons, the cross-correlogram should scatter around a null value equal to  $R_B$ , the average rate of the non-reference neuron. Deviations of the cross-correlogram from the null value result from direct or indirect interactions between the neurons. Direct interactions include monosynaptic excitatory or inhibitory interactions, which lead to short-latency peaks or troughs in the cross-correlogram, usually lasting only a few ms (Fig. 2A; Moore et al., 1970); only excitatory peaks (EPs) were seen here. The indirect interactions are correlated rate changes in two neurons produced by a shared stimulus or by common synaptic input from other neurons. These produce a symmetric peak in the cross-correlogram centered near zero delay with a width comparable to the temporal extent of the interaction (Fig. 2B).

The cross-correlogram in Fig. 2A shows an EP (shaded) between an AN fiber (the reference, presumed presynaptic) and a VCN chopper neuron. The EP is an elevation in the discharge probability of the presumed postsynaptic (VCN) neuron immediately following spikes in the reference (AN) neuron. This is the feature expected of a monosynaptic excitatory synapse, and EPs are interpreted in that way here. The peak is characterized by a short latency, consistent with a synaptic delay, a rapid rise and a somewhat longer decay. In AN–VCN pairs, EPs had latencies of  $0.46 \pm 0.29$  ms on average and durations of  $2.14 \pm 0.99$  ms (mean  $\pm$  S.D.).

The area under the EP, shaded in Fig. 2A, is called the *effectiveness* (Levick et al., 1972); it corresponds to the average number of extra spikes in the presumed postsynaptic neuron following each spike in the reference neuron. The effectiveness is a measure of the functional strength of the interaction.

Fig. 2B shows a cross-correlogram of the spike trains of two AN fibers responding to a frozen noise stimulus. The correlogram contains a central mound (CM), an approximately symmetric elevation centered on the ordinate. A CM is expected in cases where the two neurons are firing in a correlated fashion due to shared synaptic input or (as in this case) in response to a stimulus. The nature of CM is made clear by the correlogram predictor plotted as the dashed line. This is a cross-correlogram computed with a delay of one period of the frozen noise. It thus captures the

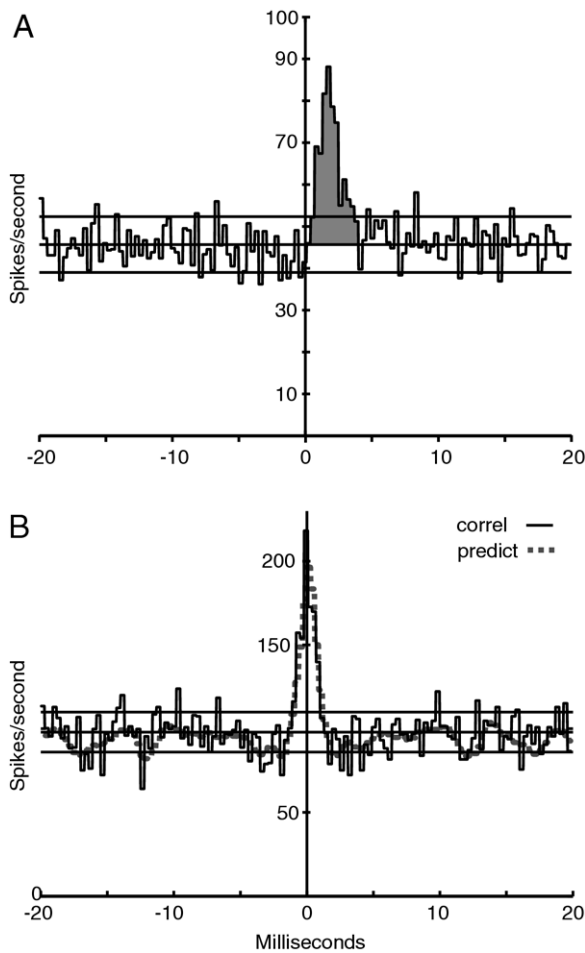


**Fig. 2.** (A) Cross-correlogram of an AN fiber (the reference neuron) and a CN chopper neuron. The ordinate is an estimate of the discharge rate of the CN neuron as a function of time relative to spikes in the AN fiber, computed in bins of 0.3 ms. The horizontal lines show the mean  $\pm 2$  standard deviations for the portion of the correlogram outside the feature. The feature (shaded) is an EP; the *effectiveness* is the area between the mean correlogram value (middle horizontal line) and the peak over the time range defined by the first zero crossings moving away from the center of the feature. In this case, *effectiveness* = 0.073. The BFs were 9.5 (AN) and 9.88 (CN) kHz. The stimulus was a continuous tone of 9.5 kHz, 4 dB SPL,  $\sim 5$  dB re threshold for the AN fiber and 10 dB re threshold for the CN neuron. (B) The solid line shows a cross-correlogram of two AN fibers, with the same parameters as in A. The fibers have BFs 4.24 and 4.38 kHz, both high spontaneous rate, and the stimulus is a frozen noise approximately 15 dB above threshold; the dotted line shows a correlogram predictor with a 1 s shift, equal to one cycle of the frozen noise stimulus. The peak centered on zero is a CM, consistent with correlation induced by the stimulus.

correlation induced by the responses to the noise without showing direct interactions between the neurons. In this case, the predictor and cross-correlogram are almost identical, showing that the CM is due to the similar responses of the two fibers (which had similar BFs) to the stimulus.

When frozen noise was used as the stimulus, a CM was observed for all AN/AN neuron pairs with BFs close enough that the neurons' frequency tuning overlapped. For AN/CN pairs, a CM was also observed with frozen noise,

but it was shifted to positive delays, consistent with the longer latency of the CN neuron. These results are expected because the neurons were responding to the envelope of the narrowband noise that results from cochlear filtering of the frozen noise signal. Thus, any two neurons with similar BFs would have correlated rate changes, because of the shared stimulus components in overlapping portions of their frequency response areas. These rate changes are evident in PST histograms of the neurons' responses to the noise (not shown). Of course, such correlograms are not useful in inferring properties of neural connections, and those data are not considered further. Spontaneous activity and continuous tones do not produce such shared rate fluctuations, because they have no envelope or a flat envelope, and so should not produce this artifactual correlation.

### Frequency extent of interaction

The cross-correlograms of AN/CN pairs are most simply interpreted if the AN fibers discharge independently of one another. If, for example, the AN fibers connected to the same hair cell (Lieberman, 1980) discharged in a correlated fashion, then a cross-correlogram feature observed between one of those fibers and a CN neuron could have been produced by an anatomical connection between any of the fibers and the CN neuron. Pairs of AN fibers were tested for cross-correlation using spontaneous and tone-evoked spike trains; tone-driven activity was included only for tones above 3 kHz to reduce the effects of phase locking (Johnson and Kiang, 1976). No significant features were seen in the cross-correlograms of 23 AN/AN pairs. A histogram of the ratios of the BFs of these pairs is shown in Fig. 3A. Because correlation is most likely in pairs with similar BFs, the electrodes were manipulated to equate the BFs of the two fibers of a pair whenever possible. Most pairs had BFs within 20%. One additional AN/AN pair with equal BFs ( $\sim 8.46$  kHz) showed a one-bin-wide apparent CM for spontaneous activity. However, the CM was not repeatable in three repetitions of the data acquisition and it was judged to be a statistical anomaly. The lack of correlation in pairs of fibers with BF ratios between 0.8 and 1 is consistent with similar results from Johnson and Kiang (1976) who report no significant correlation in about 15 pairs with similar BF ratios (their Fig. 9).

The cross-correlograms of AN/CN pairs were either featureless or showed EPs. With two exceptions, EPs were observed only for pairs with BF ratios (AN/CN) between 0.85 and 1.15 (Fig. 3C). Fig. 3B shows the BF ratios of uncorrelated pairs. Again, the focus was on pairs with similar BFs, but pairs were tested over a wide enough BF range that it is clear that EPs are confined to nearly-equal BF pairs. In fact, the probability of EP occurrence in pairs with BF ratios within 0.95–1.05 (the central bin in Fig. 3B and 3C) was significantly different from the probability in pairs with larger or smaller BF ratios (chi-square,  $P < 10^{-6}$ ); the same was true of pairs with BF ratios between 0.85–1.15, the central three bins.

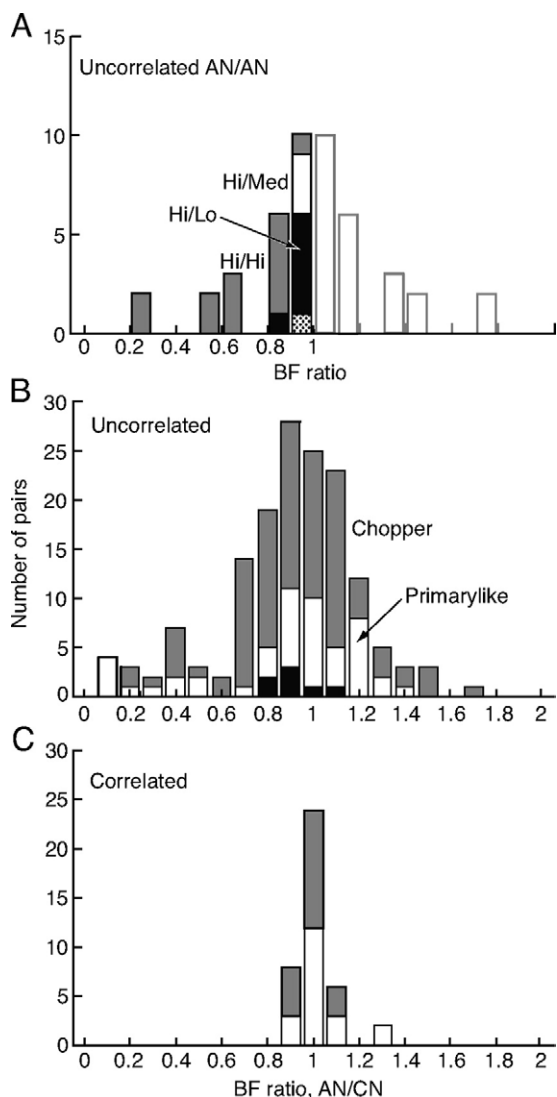


**Fig. 3.** (A) Histogram of the ratio of the BFs of all AN/AN pairs for which cross-correlograms were computed from either spontaneous or tone-driven spike trains. None of them showed significant features. The abscissa shows the ratio of the lower to the higher BF and the histogram is repeated (shaded) on the right for comparison with parts B and C. The spontaneous rate categories of the fibers are indicated by the shading, as identified by the labels. The one unidentified box in the 0.9–1 bin (dotted) is for a pair of medium spontaneous rate neurons. In cases where tone-driven activity was used, the tone frequency was above 3 kHz. (B) Ratios of the BFs (AN/CN) of all AN–VCN pairs in which all cross-correlograms showed no features. Correlograms were based on spontaneous rates whenever possible. The VCN response type is indicated by the shading. The black boxes near the abscissa are onset neurons in which enough spikes could be gathered to compute cross-correlograms. (C) Ratios of the BFs of AN–VCN pairs in which EPs were observed in at least one cross-correlogram. Shading is the same as in B.

### EPs are smaller at higher sound levels

Data were taken with spontaneous activity whenever possible and then over a range of sound levels beginning a few dB above threshold. Usually EPs could only be observed at sound levels within about 20–30 dB of threshold. Fig. 4 shows an example for a chopper neuron. The PST histogram

of the VCN neuron is shown in Fig. 4A, showing clear chopping. Three cross-correlograms with significant EPs are shown in Figs. 4B–4D for tones at the BF of the AN fiber at various levels re threshold (2–12 dB). The effectiveness declines at the highest level tested. The neurons were not held long enough to test at a higher level.

Similar data for a pri-N neuron are shown in Fig. 5. In this case, data were taken with spontaneous activity (Fig. 5B) and for tone-driven activity at 4, 9, and 14 dB re the AN threshold (Fig. 5C–5E). Again effectiveness declines with level for levels above threshold. Indeed, it is not clear that the correlogram in Fig. 5E actually has an EP, and the effectiveness is computed over the same range used for the other correlograms (0.1–2.5 ms).

Comparison of Figs. 4 and 5 shows that the latencies and durations of the EPs are longer for the chopper than the pri neuron, which was a consistent finding. Latencies were measured at the first sharp rise in the EP, but only for EPs like Figs. 4B, 4C, 5C, and 5D that had clear onsets. The latencies were  $0.63 \pm 0.30$  ms (mean  $\pm$  S.D.) for 16 chopper neurons and  $0.31 \pm 0.19$  ms for 18 pri neurons ( $P \sim 0.002$ , rank sum test). Durations of the EPs were also different,  $2.66 \pm 0.90$  ms for choppers and  $1.68 \pm 0.55$  ms for pri neurons ( $P < 0.001$ , rank sum test).

The decrease in the functional strength of the EP is shown for the whole population in Fig. 6. A and C of this figure show effectiveness plotted against the sound level. A second measure, contribution, is plotted in B and D; contribution is the area of the EP in a cross-correlogram computed with the VCN neuron as the reference. It is thus the average number of times a spike in the presumed postsynaptic neuron is preceded by a spike in the AN fiber under study, and so it is the average contribution of the AN fiber to a spike in the VCN neuron. Because the cross-correlograms obtained with the two choices of reference neuron are the same except for the normalization ( $N_A$  in the denominator of Eqn. 1), contribution is related to effectiveness by the ratio  $N_{AN}/N_{VCN}$ . The two measures convey slightly different aspects of neural interactions, but do not differ dramatically here because  $N_{AN}/N_{VCN} \sim 1$  in most cases.

Fig. 6 shows that EP features were observed in cross-correlograms only within about 20 dB of the AN threshold (and at similar levels for the VCN neurons because thresholds are about the same). Sometimes data were taken at higher sound levels, but there were no significant features in the cross-correlograms so those data do not appear in Fig. 6. Thus even though a VCN neuron responds strongly to the stimulus at sound levels  $>20$  dB above threshold, the relationship of single AN and VCN spikes, as it is revealed in the cross-correlogram, is lost.

The dependence of correlation on sound level raises the question of the effects of low and medium spontaneous rate fibers with higher thresholds. In one model of cochlear nucleus processing, it was hypothesized that responses of VCN neurons would shift from being dominated by high spontaneous rate (low threshold) AN fibers at low sound levels to low spontaneous rate (high threshold) fibers at high sound levels (Lai et al., 1994). However, the present

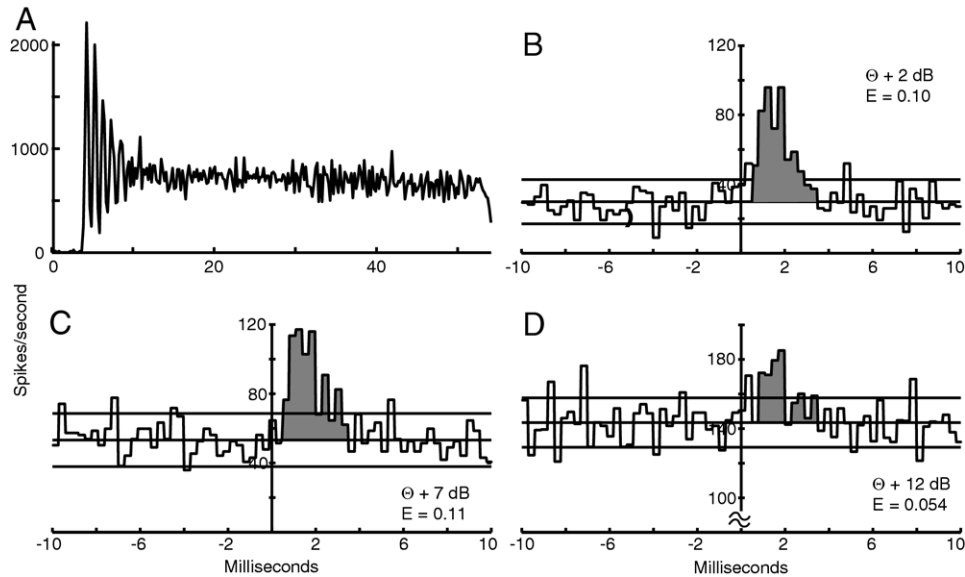


**Fig. 4.** (A) PST histogram of the responses of a chopper neuron to 9.0 kHz (BF) tone bursts at 24 dB re threshold. (B–D) Cross-correlograms of this neuron's spike trains with a high spontaneous rate AN fiber (BF=9.0 kHz) at three sound levels, given as dB re the AN threshold ( $\theta$ ). The threshold of the chopper neuron was 4 dB below that of the AN fiber. The shaded areas show the EPs; effectiveness values are given on the plots. The range of the EP (shaded) was chosen to extend from the sharp rise of the EP to the first zero crossing in B and C and the same range was used in D. The correlograms were computed with 0.3 ms bins and the PST histogram with 0.2 ms bins.

data provide no support for this hypothesis. The likelihood, as a function of sound level, of observing an EP in a cross-correlogram appears to be the same for all three spontaneous rate groups (not shown). In fact, because low spontaneous rate fibers have high thresholds, they were mainly tested at levels substantially above the threshold of the VCN neuron (median 22 dB re CN threshold), levels at which medium and high spontaneous rate fibers show small or no significant features. Only one cross-correlogram (1/28) containing a low spontaneous rate fiber showed a significant EP (at 13 dB re the threshold of the primarylike CN neuron).

### Interspike interval conditioning

The cross-correlogram measures a direct effect of individual AN spikes on spikes in the VCN neuron. It is also possible to investigate second-order effects, meaning whether an AN spike is more or less effective if immediately preceded by another AN spike. Such effects might be expected, for example, because of short-term synaptic plasticity, either depression or facilitation (e.g. Xu et al., 2007). Such effects would show up as changes in the effectiveness of the EP as a function of the interspike interval from the reference spike to the previous spike in the AN fiber. Large effects of this kind are seen in monosynaptic or disynaptic connections from retina to visual cortex (Kara and Reid, 2003).

Fig. 7A shows a conditional histogram in which the AN spikes used to construct the cross-correlogram were required to be preceded by another AN spike at an interval of 4–8 ms, shown by the brackets just below the correlogram. The EP from the unconditioned cross-correlogram is shown shaded and the conditioned correlogram is shown

by solid lines. The effect of the conditioning is evident at negative latencies (between about  $-6$  and  $0$  ms) where the conditioned correlogram has a substantial elevation, reflecting the CN neuron's response to the first spike of the pair. The effect of the conditioning was to increase slightly the EP area in response to the second spike of the pair, from an effectiveness of about 0.088 in the unconditioned case to 0.099. The opposite effect is seen in Fig. 7B where the conditioning required that the AN spikes be preceded by no other AN spike for at least 8 ms. The effect of the conditioning in this case is a clear decrease in the correlogram at negative latencies and a reduction in the size of the EP, to an effectiveness of 0.066. Note that these effects are opposite to the effects expected from postsynaptic refractoriness, which should decrease the EP in Fig. 7A and increase it in Fig. 7B. They are thus consistent with weak presynaptic facilitation, increased in Fig. 7A and decreased in Fig. 7B.

The test shown in Fig. 7 could be done on 14 cross-correlograms that had a sufficient number of presynaptic spikes to support conditioning and large enough EPs to allow small effects to be observed. No conditioning effects were seen in four cases in pri neurons and small effects like Fig. 7 were seen in 4 of 10 choppers. Thus the effects of spike conditioning are at best subtle under the conditions of this experiment.

## DISCUSSION

### General comments

The results of this paper show that AN fibers form short latency, rapidly acting excitatory synapses on VCN neurons. The connections are strongly tonotopic and can only

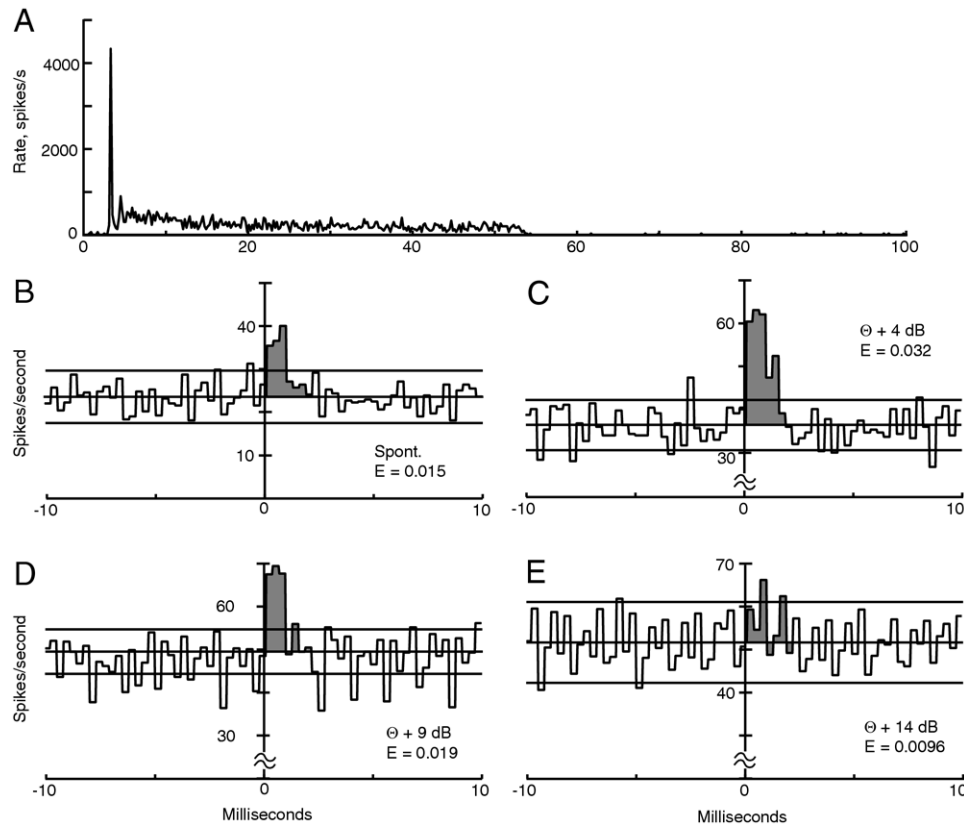


**Fig. 5.** (A) PST histogram of the responses of a pri-N neuron to 6.50 kHz (BF) tone bursts at 30 dB re threshold. (B–E) Cross-correlograms of this neuron's spike trains with a high spontaneous rate AN fiber (BF=6.82 kHz) for spontaneous activity and three sound levels, given as dB re the AN threshold ( $\theta$ ). The threshold of the pri-N neuron was the same as the AN fiber. The shaded areas show the EPs; effectiveness values are given on the plots. The range of the EP (shaded) was chosen to be the same in E as in the other three cases, where the peak is clear. The correlograms were computed with 0.3 ms bins and the PST histogram with 0.2 ms bins.

be observed in a cross-correlogram for sound levels within about 20 dB of threshold (for steady-tone-driven or spontaneous activity). The EPs are similar for pri and chopper neurons, except that latencies and durations are shorter for pri neurons.

The duration of the EPs suggests that the AN–VCN synapse operates rapidly with a postsynaptic effect on spiking probability that lasts only about 1–4 ms. The EP should correspond roughly to the derivative of the excitatory postsynaptic potential (EPSP) in the postsynaptic cell (Knox and Poppele, 1977) and therefore its duration should match the rise time of the EPSP or the duration of the current injected by the synapse (the excitatory postsynaptic current, EPSC). The glutamate receptors in VCN neurons are among the fastest known (Raman and Trussell, 1992; Gardner et al., 2001), producing EPSCs that last only  $\sim 1$  ms in VCN neurons, similar to VCN synaptic rise times with electrical stimulation of the AN (Paolini and Clark, 1998). Thus the EPs are somewhat longer than expected from the intracellular data.

We assume that the EP represents a direct synaptic effect of the AN fiber on the VCN neuron. One possible alternative to this interpretation is that AN fibers discharge in a correlated way with other fibers of similar BF, and the EP represents the cumulative effect of a population of such

correlated fibers on the VCN neuron. Two observations argue against this alternative interpretation. The first is that no such correlation between AN fibers was observed here, consistent with previous work by Johnson and Kiang (1976). The second is that the EPs differ in important ways between spontaneous or tone-driven activity versus noise-driven activity. EPs in response to noise are observed in essentially all AN–VCN pairs with overlapping tuning, as opposed to 33–50% of the cases for spontaneous activity or tone-driven responses. Moreover, EPs of noise-driven responses decline with sound level much less than in Fig. 6, with essentially no decline in choppers; for noise, EPs were observed at all levels tested up to 40 dB re threshold. The difference is that noise produces a stimulus-driven response of AN fibers to the envelope of the noise and this response is correlated across fibers with overlapping tuning (evident in PST histograms and correlogram predictors like Fig. 2B). As a result, VCN neurons respond to the summated effect of the correlated AN inputs, which produces a postsynaptic membrane potential that is similar to the envelope of the noise and is also correlated with the AN fibers' spike rates. This behavior is not seen in spontaneous or tone-driven responses because the fibers discharge independently with no particular temporal pattern and the postsynaptic response has no particular temporal

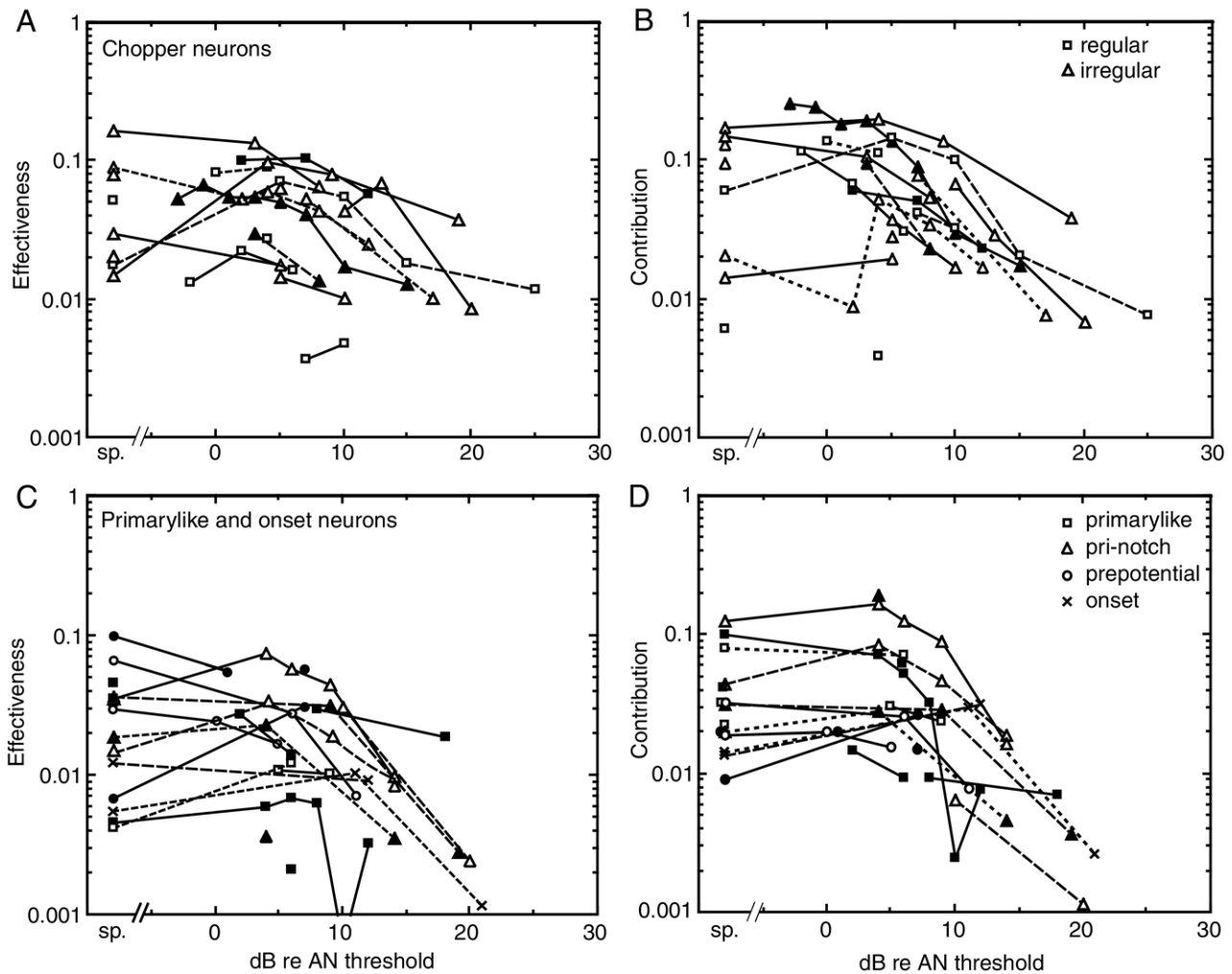


**Fig. 6.** The effectiveness and contribution of EPs between AN fibers and VCN neurons are plotted against the sound level of the stimulus tone, as dB re the threshold of the AN fiber. Data for spontaneous activity are plotted to the left of the break in the abscissa. (A, B) Data from choppers. (C, D) Data from pri and onset neurons. Data from different subclasses of neurons are shown with different symbol shapes, identified in the legends. For the choppers, these correspond to chop-S (regular) and chop-T (irregular; Young et al., 1988). Some pri neurons are identified only as “prepotential” neurons; these were cases with no PST histogram data, but a noticeable prepotential in the action potential, marking them as pri neurons (Pfeiffer, 1966; Guinan and Li, 1990). Data from three onset neurons are also plotted. The different line styles and symbol filling are used to differentiate data from different neurons and have no other meaning.

features. It is important to this argument that all the pairs studied here had BFs above 3 kHz, so there was little or no phase locking to tones.

A second alternative interpretation is that the EPs result from disynaptic EPSPs (Ferragamo et al., 1998), say due to collaterals of T-stellate neurons (likely choppers) that distribute in VCN (Smith and Rhode, 1989; Oertel et al., 1990). However the short latencies of the EPs observed here make a disynaptic circuit unlikely, and the direct AN–CN connection is a more parsimonious explanation.

#### Lack of short-term synaptic plasticity

The interval-conditioning analysis (Fig. 7) showed little effect of short-term synaptic plasticity. Whether such effects are expected is unclear. The calyx of Held synapses in the auditory brainstem do show synaptic depression and

facilitation (reviewed in Xu et al., 2007), although apparently these effects are smaller in the cochlear nucleus of mature animals (Wu and Oertel, 1987; Brenowitz and Trussell, 2001). Relatively small synaptic depression effects are seen in bushy cells (Wang and Manis, 2006); in non-bushy cells, depression and facilitation seem to overlap, giving a small net effect (MacLeod et al., 2007). In addition, there are important differences between *in vivo* and slice experiments (Hermann et al., 2007). *In vivo*, AN fibers are spontaneously active at rates from 0 to ~100/s and the majority of them have spontaneous rates above 20/s; they discharge in an irregular fashion that gives an approximately exponential distribution of interspike intervals, in which short intervals are most common but intervals vary widely. This is especially so in real world conditions where there is background sound, so that a fiber is often active at rates above its spontaneous rate. Given the

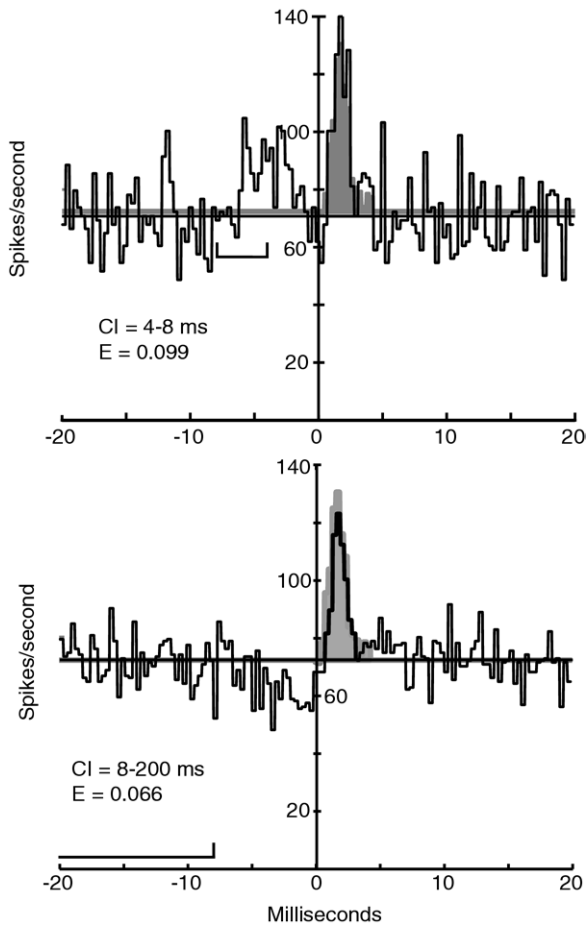


**Fig. 7.** Cross-correlograms between an AN fiber and a VCN chopper neuron computed with conditions on the interspike interval preceding the AN spike. For both, the brackets in the left half of the plot show the conditioning interval. (A) The reference AN spike was preceded by another AN spike at an interval of 4–8 ms. Note the response to the conditioning spike for latencies of  $-6$ – $0$  ms. This manipulation might strengthen synaptic facilitation or depression. (B) The reference spike was not preceded by another spike for a duration of at least 8 ms, which should reduce any facilitation or depression. In each case the conditional histogram is shown by solid lines and the EP of the unconditioned cross-correlogram is shown shaded. Only the EP of the unconditioned histogram is shown, the remainder of that cross-correlogram is suppressed. The conditioning interval (CI) and effectiveness (E) of the EPs in the conditioned histograms are shown on the plots. The unconditioned effectiveness was 0.088. The effectiveness in both cases is computed relative to the reference (mean) level of the unconditioned cross-correlogram.

time constants usually described for short-term plasticity, most AN synapses should be in a steady state for the processes involved in both facilitation and depression under *in vivo* conditions (Hermann et al., 2007; P. B. Manis, personal communication).

Thus short-term synaptic plasticity is not likely to have the large effects *in vivo* that are seen in intracellular recording experiments in slice. This reasoning may not apply to synapses made by low spontaneous rate fibers for stimuli that fluctuate substantially in amplitude over time scales of tens of ms, like speech in a quiet background. Despite that reservation, our results suggest that short-

term synaptic plasticity in AN–VCN synapses contributes little to synaptic strengths under the stimulus conditions used here.

### The operating mode of VCN neurons at high sound levels

The decline in the effectiveness of EPs as sound level increases (Fig. 6) shows that the direct relationship between presynaptic and postsynaptic spikes that is usually postulated for AN–VCN neurons only holds near threshold. This suggests that VCN neurons operate in two different integrating modes, depending on the sound level. At low levels, they behave like the common integrate and fire neuron model in which EPSPs are summed and spikes are produced when the summation crosses a threshold, followed by a resetting of membrane potential to rest (e.g. the model of Arle and Kim, 1991). In this model, the threshold crossing must occur just after a spike in one of the presynaptic neurons, because that is the only time when the postsynaptic potential increases to cross threshold. Thus EPs should be observed at all sound levels, different from the result in Fig. 6. The second integrating mode, at high sound levels, consists of the postsynaptic neuron firing in response to the integrated overall input, in an oscillating mode or limit cycle that is determined by the properties of the postsynaptic membrane and not by the pattern of synaptic inputs. This type of response occurs, for example, if the summated membrane potential goes above the spiking threshold and is maintained there by the synaptic inputs, which occurs in chopper neurons during short tone bursts (Smith and Rhode, 1989; Paolini et al., 2005). A Hodgkin-Huxley style model of chopper neurons behaves in this way and shows a loss of EPs at high discharge rates (Sachs et al., 1993).

However, such a mode of operation (autonomous oscillation) seems to require a regular discharge from the neuron, in which the variance of the interspike intervals is small. Regular discharge is a defining characteristic of chopper neurons and is observed in responses to short tone bursts, including in the choppers studied here. However, calculations of interspike-interval statistics for our cross-correlation data showed irregular discharges (coefficient of variation near 1.0) in almost all cases, including cases in which the EP disappeared. Such irregular discharges have been reported for chopper neurons responding to vowel stimuli at low and high sound levels (May et al., 1998) suggesting that irregular discharge is the normal encoding mode of chopper neurons for stimuli other than short tones. Thus if the explanation for the loss of the EP at high sound levels is to be an autonomous oscillation, the oscillation has to have a chaotic character, perhaps because of the randomness of the summated suprathreshold synaptic drive. Clearly, the nature of the responses of chopper neurons to suprathreshold stimuli requires further work.

One alternative interpretation of the loss of EPs at high levels is inhibitory inputs timed to precisely overlap with excitatory inputs; if the inhibitory inputs were driven only at high sound levels, then they could conceivably reduce the

postsynaptic EPSPs. Inhibitory inputs from D-stellate neurons are a possible candidate (Smith and Rhode, 1989; Ferragamo et al., 1998). However, inhibitory cross-correlograms were not observed in this data set. Moreover, the discharge rates of the CN neurons usually increased with sound level (as in Figs. 4 and 5), rather than decreasing as the inhibitory cancellation model seems to require. Thus inhibitory inputs seem to be an unlikely explanation.

A second alternative is that VCN neurons receive numerous small synaptic inputs and small numbers of large ones. In this case, the large synaptic inputs may come to dominate the neuron's responses at high sound levels, which could lead to the results reported here if the recordings are exclusively from the small inputs. While such a synaptic arrangement is likely in bushy cells (e.g. Ryugo and Fekete, 1982; Liberman, 1991) and has been shown to be consistent with some aspects of phase locking in pri neurons (Rothman and Young, 1996; Zhang and Carney, 2005), there is little evidence for it in multipolar neurons.

It is interesting that EPs are not observed in cross-correlograms of AN fibers and neurons in DCN (Sydorenko, 1992), even under conditions where they are observed in VCN. This result may indicate that DCN neurons always operate in one of the postulated high-sound-level modes. It could also mean that DCN neurons receive weak AN inputs, as suggested from fiber reconstructions (Ryugo and May, 1993), and are actually driven disynaptically by collaterals of VCN multipolar cells (Evans and Nelson, 1973; Smith and Rhode, 1989); EPs would be unobservable in this case, because their effectiveness should be the square of the effectiveness reported here for VCN neurons.

### Pri versus chopper responses

The contribution values in Fig. 6B and 6D suggest that each AN fiber contributes less than 10–20% to the average postsynaptic spike. In chopper neurons, this result is not surprising, in that such neurons have long been considered to integrate activity across a number of AN fibers (e.g. Molnar and Pfeiffer, 1968). The number of independent AN fiber terminals on a VCN multipolar cell is not known, because the terminals are mainly on dendritic trees. However, by analysis of the distribution of the amplitudes of EPSPs, it has been estimated that such cells receive about five independent AN inputs (Ferragamo et al., 1998). The results here suggest that more AN inputs would be needed, more like 10–20; however, it is doubtful that either technique is accurate enough produce a precise estimate of the number of weak synapses, so these estimates should not be considered to be in disagreement.

The results for pri-notch neurons, which correspond to globular bushy cells (Smith and Rhode, 1987), also correspond reasonably well to what is known about these cells. Estimates of the number of AN synapses on a globular bushy cell vary from ~15 to ~60 (Liberman, 1991; Ostapoff and Morest, 1991; Spirou et al., 2005). These numbers correspond to the effectiveness values in Fig. 6, assuming a range of synaptic strengths among the terminals contacting a cell.

For pri neurons, however, the presence of only weak EPs in our data is surprising. Spherical bushy cells receive terminals from one to four AN fibers as large end bulbs (Osen, 1970a; Ryugo and Sento, 1991; Nicol and Walmsley, 2002). Pri neurons that receive such synaptic terminals seem to fire action potentials with high probability in response to single AN spikes, based on analysis of complex action potentials in the VCN (i.e. prepotentials; Pfeiffer, 1966; Kopp-Scheinflug et al., 2002). Clearly such AN–VCN pairs were not included in our data, because they would have shown contribution values of 0.25 or more. The largest end bulbs are seen for lower BFs (<4 kHz in cat, Rouiller et al., 1986), which we avoided in our recordings. Nevertheless, end bulbs are seen at all BFs, as are prepotentials, so it is unlikely that BF choice explains the lack of end bulb-like recordings. More likely, the explanation is simply that the probability of recording such a pair is very small. About half the EPs in Fig. 6D are from neurons that are likely to be spherical bushy cells, based on their PST histograms and other properties, and those EPs have small amplitudes, comparable to choppers. These small inputs to pri neurons may reflect the presence of small non-end bulb synapses on spherical bushy cells. Such small synapses have been described in electron-microscopic studies (Ryugo and Sento, 1991), but no potential physiological correlate has been described previously.

### Final comments

The most unexpected finding in this paper is the loss of EPs at sound levels only 20 dB into the dynamic range of the auditory system. This demonstrates clearly the importance of the properties of the postsynaptic membrane in cochlear nucleus neurons. For bushy cells, the fast membrane time constants are well understood and appreciated (e.g. McGinley and Oertel, 2006). However, for choppers the present results raise the question of what determines the postsynaptic response characteristics for stimuli at high enough levels to drive the system out of its 1:1 spiking mode with AN fibers. Perhaps this question will provide a way to further explore the large set of potassium channels observed in VCN neurons (Rothman and Manis, 2003; Cao et al., 2007), which otherwise seems to be more than is required for current concepts of synaptic integration in those neurons.

*Acknowledgments*—Preparation of this manuscript was aided by conversations with Sharba Bandyopadhyay, Philip Joris, Wei-Li Ma, Paul Manis, Paul Nelson, Donata Oertel, and Josh Vogelstein, along with the comments of two anonymous reviewers. The technical support of Ron Atkinson and Phyllis Taylor is appreciated.

### REFERENCES

- Arle JE, Kim DO (1991) Neural modeling of intrinsic and spike-discharge properties of cochlear nucleus neurons. *Biol Cybern* 64: 273–283.
- Banks MI, Sachs MB (1991) Regularity analysis in a compartmental model of chopper units in the anteroventral cochlear nucleus. *J Neurophysiol* 65:606–629.

- Blackburn CC, Sachs MB (1989) Classification of unit types in the anteroventral cochlear nucleus: PST histograms and regularity analysis. *J Neurophysiol* 62:1303–1329.
- Blackburn CC, Sachs MB (1990) The representation of the steady-state vowel sound /e/ in the discharge patterns of cat anteroventral cochlear nucleus neurons. *J Neurophysiol* 63:1191–1212.
- Brenowitz S, Trussell LO (2001) Maturation of synaptic transmission at end-bulb synapses of the cochlear nucleus. *J Neurosci* 21:9487–9498.
- Cant NB (1992) The cochlear nucleus: Neuronal types and their synaptic organization. In: *The mammalian auditory pathway: neuroanatomy* (Webster DB et al., eds), pp 66–116. Berlin: Springer-Verlag.
- Cao XJ, Shatadal S, Oertel D (2007) Voltage-sensitive conductances of bushy cells of the mammalian ventral cochlear nucleus. *J Neurophysiol* 97:3961–3975.
- deCharms RC, Merzenich MM (1996) Primary cortical representation of sounds by the coordination of action-potential timing. *Nature* 381:610–613.
- Eggermont JJ (2006) Properties of correlated neural activity clusters in cat auditory cortex resemble those of neural assemblies. *J Neurophysiol* 96:746–764.
- Evans EF, Nelson PG (1973) On the functional relationship between the dorsal and ventral divisions of the cochlear nucleus of the cat. *Exp Brain Res* 17:428–442.
- Ferragamo MJ, Golding NL, Oertel D (1998) Synaptic inputs to stellate cells in the ventral cochlear nucleus. *J Neurophysiol* 79:51–63.
- Gardner SM, Trussell LO, Oertel D (2001) Correlation of AMPA receptor subunit composition with synaptic input in the mammalian cochlear nuclei. *J Neurosci* 21:7428–7437.
- Goldstein JL, Baer T, Kiang NYS (1971) A theoretical treatment of latency, group delay, and tuning characteristics for auditory-nerve responses to clicks and tones. In: *Physiology of the auditory system* (Sachs MB, ed), pp 133–142. Baltimore: National Educational Consultants, Inc.
- Guinan JJ, Li RY-S (1990) Signal processing in brainstem auditory neurons which receive giant endings (calyces of Held) in the medial nucleus of the trapezoid body of the cat. *Hear Res* 49:321–334.
- Hermann J, Pecka M, von Gersdorff H, Grothe B, Klug A (2007) Synaptic transmission at the calyx of Held under in vivo-like activity levels. *J Neurophysiol* 98:807–820.
- Hewitt MJ, Meddis R (1993) Regularity of cochlear nucleus stellate cells: A computational modeling study. *J Acoust Soc Am* 93:3390–3399.
- Johnson DH, Kiang NYS (1976) Analysis of discharges recorded simultaneously from pairs of auditory nerve fibers. *Biophys J* 16:719–734.
- Joris PX, Carney LH, Smith PH, Yin TCT (1994) Enhancement of neural synchronization in the anteroventral cochlear nucleus. II: Responses in the tuning curve tail. *J Neurophysiol* 71:1037–1051.
- Joris PX, Yin TCT (2007) A matter of time: internal delays in binaural processing. *Trends Neurosci* 30:70–78.
- Joris PX, Smith PH (2008) The volley theory and the spherical cell puzzle. *Neuroscience* 154:65–76.
- Kara P, Reid RC (2003) Efficacy of retinal spikes in driving cortical responses. *J Neurosci* 23:8547–8557.
- Knox CK, Poppele RE (1977) Correlation analysis of stimulus-evoked changes in excitability of spontaneously firing neurons. *J Neurophysiol* 40:616–625.
- Kopp-Scheinflug C, Dehmel S, Dorrscheidt GJ, Rubsamen R (2002) Interaction of excitation and inhibition in anteroventral cochlear nucleus neurons that receive large endbulb synaptic endings. *J Neurosci* 22:11004–11018.
- Lai YC, Winslow RL, Sachs MB (1994) A model of selective processing of auditory-nerve inputs by stellate cells of the antero-ventral cochlear nucleus. *J Comput Neurosci* 1:167–194.
- Levick WR, Cleland BG, Dubin MW (1972) Lateral geniculate neurons of cat: Retinal inputs and physiology. *Invest Ophthalmol* 11:302–311.
- Lieberman MC (1980) Morphological differences among radial afferent fibers in the cat cochlea: an electron-microscopic study of serial sections. *Hear Res* 3:45–63.
- Lieberman MC (1991) Central projections of auditory-nerve fibers of differing spontaneous rate. I. Anteroventral cochlear nucleus. *J Comp Neurol* 313:240–258.
- Louage DH, van der Heijden M, Joris PX (2005) Enhanced temporal response properties of anteroventral cochlear nucleus neurons to broadband noise. *J Neurosci* 25:1560–1570.
- MacLeod KM, Horiuchi TK, Carr CE (2007) A role for short-term synaptic facilitation and depression in the processing of intensity information in the auditory brain stem. *J Neurophysiol* 97:2863–2874.
- Manis PB, Marx SO (1991) Outward currents in isolated ventral cochlear nucleus neurons. *J Neurosci* 11:2865–2880.
- May BJ, LePrell GS, Sachs MB (1998) Vowel representations in the ventral cochlear nucleus of the cat: Effects of level, background noise, and behavioral state. *J Neurophysiol* 79:1755–1767.
- McGinley MJ, Oertel D (2006) Rate thresholds determine the precision of temporal integration in principal cells of the ventral cochlear nucleus. *Hear Res* 216:52–63.
- Miller LM, Escabi MA, Read HL, Schreiner CE (2001) Functional convergence of response properties in the auditory thalamocortical system. *Neuron* 32:151–160.
- Molnar CE, Pfeiffer RR (1968) Interpretation of spontaneous spike discharge patterns of cochlear nucleus neurons. *Proc IEEE* 56:993–1004.
- Moore GP, Segundo JP, Perkel DH, Levitan H (1970) Statistical signs of synaptic interaction in neurons. *Biophys J* 10:876–900.
- Nicol MJ, Walmsley B (2002) Ultrastructural basis of synaptic transmission between endbulbs of Held and bushy cells in the rat cochlear nucleus. *J Physiol* 539:713–723.
- Oertel D (1983) Synaptic responses and electrical properties of cells in brain slices of the mouse anteroventral cochlear nucleus. *J Neurosci* 3:2043–2053.
- Oertel D, Wu SH, Garb MW, Dizack C (1990) Morphology and physiology of cells in slice preparations of the posteroventral cochlear nucleus of mice. *J Comp Neurol* 295:136–154.
- Osen KK (1969) Cytoarchitecture of the cochlear nuclei in the cat. *J Comp Neurol* 136:453–482.
- Osen KK (1970a) Afferent and efferent connections of three well-defined cell types of the cat cochlear nucleus. In: *Excitatory synaptic mechanisms* (Anderson P, Jansen JKS, eds), pp 295–300. Oslo: Universitetsforlaget.
- Osen KK (1970b) Course and termination of the primary afferents in the cochlear nuclei of the cat. *Arch Ital Biol* 108:21–51.
- Ostapoff EM, Feng JJ, Morest DK (1994) A physiological and structural study of neuron types in the cochlear nucleus. II. Neuron types and their structural correlation with response properties. *J Comp Neurol* 346:19–42.
- Ostapoff EM, Morest DK (1991) Synaptic organization of globular bushy cells in the ventral cochlear nucleus of the cat: A quantitative study. *J Comp Neurol* 314:598–613.
- Paolini AG, Clark GM (1998) Intracellular responses of the rat anteroventral cochlear nucleus to intracochlear electrical stimulation. *Brain Res Bull* 46:317–327.
- Paolini AG, Clarey JC, Needham K, Clark GM (2005) Balanced inhibition and excitation underlies spike firing regularity in ventral cochlear nucleus chopper neurons. *Eur J Neurosci* 21:1236–1248.
- Pfeiffer RR (1966) Anteroventral cochlear nucleus: Wave forms of extracellularly recorded spike potentials. *Science* 154:667–668.
- Raman I, Trussell LO (1992) The kinetics of the responses to glutamate and kainate in neurons of the avian cochlear nucleus. *Neuron* 9:173–186.

- Rhode WS (2008) Response patterns to sound associated with labeled globular/bushy cells in cat. *Neuroscience* 154:87–98.
- Rhode WS, Oertel D, Smith PH (1983) Physiological response properties of cells labeled intracellularly with horseradish peroxidase in cat ventral cochlear nucleus. *J Comp Neurol* 213:448–463.
- Rothman JS, Manis PB (2003) The roles potassium currents play in regulating the electrical activity of ventral cochlear nucleus neurons. *J Neurophysiol* 89:3097–3113.
- Rothman JS, Young ED (1996) Enhancement of neural synchronization in computational models of ventral cochlear nucleus bushy cells. *Auditory Neurosci* 2:47–62.
- Rothman JS, Young ED, Manis PB (1993) Convergence of auditory nerve fibers onto bushy cells in the ventral cochlear nucleus: Implications of a computational model. *J Neurophysiol* 70:2562–2583.
- Rouiller EM, Cronin-Schreiber R, Fekete DM, Ryugo DK (1986) The central projections of intracellularly labeled auditory nerve fibers in cats: An analysis of terminal morphology. *J Comp Neurol* 249:261–278.
- Ryugo DK, Fekete DM (1982) Morphology of primary axosomatic endings in the anteroventral cochlear nucleus of the cat: A study of the endbulbs of Held. *J Comp Neurol* 210:239–257.
- Ryugo DK, May SK (1993) The projections of intracellularly labeled auditory nerve fibers to the dorsal cochlear nucleus of cats. *J Comp Neurol* 329:20–35.
- Ryugo DK, Sento S (1991) Synaptic connections of the auditory nerve in cats: Relationship between endbulbs of Held and spherical bushy cells. *J Comp Neurol* 305:35–48.
- Sachs MB, Wang X, Molitor SC (1993) Cross-correlation analysis and phase-locking in a model of the ventral cochlear nucleus stellate cell. In: *The mammalian cochlear nuclei: organization and function* (Merchan MA et al., eds), pp 411–420. New York: Plenum.
- Smith PH, Rhode WS (1987) Characterization of HRP-labeled globular bushy cells in the cat anteroventral cochlear nucleus. *J Comp Neurol* 266:360–375.
- Smith PH, Rhode WS (1989) Structural and functional properties distinguish two types of multipolar cells in the ventral cochlear nucleus. *J Comp Neurol* 282:595–616.
- Spirou GA, Rager J, Manis PB (2005) Convergence of auditory-nerve fiber projections onto globular bushy cells. *Neuroscience* 136:843–863.
- Sydorenko MR (1992) Analysis of functional connectivity in the cat dorsal cochlear nucleus. Ph.D. Thesis, The Johns Hopkins University.
- Voigt HF, Young ED (1990) Cross-correlation analysis of inhibitory interactions in dorsal cochlear nucleus. *J Neurophysiol* 64:1590–1610.
- Wang X, Sachs MB (1995) Transformation of temporal discharge patterns in a ventral cochlear nucleus stellate cell model: Implications for physiological mechanisms. *J Neurophysiol* 73:1600–1616.
- Wang Y, Manis PB (2006) Temporal coding by cochlear nucleus bushy cells in DBA/2J mice with early onset hearing loss. *J Assoc Res Otolaryngol* 7:412–424.
- Wu SH, Oertel D (1987) Maturation of synapses and electrical properties of cells in the cochlear nuclei. *Hear Res* 30:99–110.
- Xu J, He L, Wu LG (2007) Role of  $Ca^{++}$  channels in short-term synaptic plasticity. *Curr Opin Neurobiol* 17:352–359.
- Young ED, Robert JM, Shofner WP (1988) Regularity and latency of units in ventral cochlear nucleus: implications for unit classification and generation of response properties. *J Neurophysiol* 60:1–29.
- Zhang X, Carney LH (2005) Response properties of an integrate-and-fire model that receives subthreshold inputs. *Neural Comput* 17:2571–2601.

(Accepted 11 January 2008)  
(Available online 5 February 2008)